This is the accepted manuscript made available via CHORUS. The article has been published as:

Formation mechanism of quasiordered superstructures of electric bubbles

Maxim A. Makeev, Suyash Rijal, Yousra Nahas, Sergei Prokhorenko, and Laurent Bellaiche

Phys. Rev. B **111**, L060305 — Published 27 February 2025

DOI: 10.1103/PhysRevB.111.L060305

Formation mechanism of quasiordered superstructures of electric bubbles

Maxim A. Makeev[1]*, Suyash Rijal[1], Yousra Nahas[1], Sergei Prokhorenko[1], and L. Bellaiche[1,2]

[1] Smart Ferroic Materials Center, Physics Department, Institute for Nano-science and Engineering, University of Arkansas, Fayetteville, Arkansas 72701, United States
[2] Department of Materials Science and Engineering, Tel Aviv University, Ramat Aviv, Tel Aviv 6997801, Israel
*Corresponding Author: mmakeev@uark.edu

The phenomenon of spontaneous formation of *quasi-hexagonal arrays* of electric bubbles in systems of electric dipoles subjected to an external electric field bias is studied via *ab initio*-based simulations of ultrathin ferroelectric films. We find that the formation of such topologically non-trivial superstructures is driven by development and evolution of *soft-mode triplets* with equal wavelengths and eigen-frequencies. The *concurrent* development of these soft-modes takes place above the transition point and the soft-modes become frozen-in near the transition temperature, where frequencies of the soft-modes attain a minimum value. A further gradual cooling (or heating) of the superstructures leads to an increase in the soft-mode frequencies, following a square root law around the transition point. We quantify the thermal behavior of the degree of quasi-hexagonal ordering and find that the dipole structure factor intensities show the same critical behavior around the transition point as the soft-mode frequencies. The critical behavior, associated with the topological changes, is consistent with the Landau theory of phase transitions.

Introduction—Topologically-protected localized and extended states of matter have long been a fascinating area of research in condensed matter physics [1]. In addition to a general interest in fundamental science, associated with the phenomenon of topological pattern formation and their dynamical evolution under external electric or magnetic stimuli, these structures are regarded to be of relevance for device applications in domain-wall nanoelectronics and as a conceptual base and/or theoretical framework for design of novel memory technologies [2,3]. In this context, of particular importance are solid-state materials possessing certain types of intrinsic topological order. Such materials include certain types of magnetics, ferroelectrics, multiferroics, and complex material systems composed thereof [4]. Topological phases in the ferroelectric material systems have recently been and currently are under extensive scrutiny, and many aspects of fascinating fundamental science pertaining to polar topological structures have been unraveled in recent years [5]. Thus, it is well established by now that the electric topological texture formation is controlled by depolarization at the boundaries of ferroelectric films, strain, and strain-gradients arising from interfaces in multilayered material systems [6,7]. However, understanding of topologically non-trivial ferroelectric states is far from being complete. One of the particularly important directions of research regards *dynamical behavior* in the topologically non-trivial phases of ferroelectric material systems [8].

Electric bubbles (polar Skyrmion bubbles) comprise one class of topologically non-trivial states that emerge in ferroelectric (ultra-)thin layers. The existence of these topological states was theoretically predicted in the year of 2006 [6]. Subsequent experimental studies, performed on thin epitaxial $PbZr_{0.2}Ti_{0.8}O_3/SrTiO_3/PbZr_{0.2}Ti_{0.8}O_3$ ferroelectric sandwich structures, confirmed this prediction and provided a further characterization of these topological patterns [9]. Moreover, a similar bubble-like domains were experimentally observed in $(PbTiO_3)/SrTiO_3)_n$ superlattices grown on lattice-mismatched $SrTiO_3$ (001)-oriented substrates [10]. Noteworthy is the observation that these structures can be regarded as electric counterparts of magnetic Skyrmions (for a recent review of electric bubble (super-)structures, see Ref. [11]). Recent studies addressed various issues related to the properties of individual electric bubbles and their ensembles including studies of stability of the bubble-like polarization patterns. Specifically, the effects of depolarizing field, external electric field, film thickness, and applied pressure have been investigated in Refs. [12,13]. Importantly, the effects of thin film characteristics on transitions between different topological regimes was addressed in Ref. [12]. The issues related to ordering in polar textures, associated with transition from labyrinthine to electric bubble states were first discussed in Ref. [14]. Further, in the works of Refs. [15,16], the authors showed that a system of electric dipoles, subjected to an electric field bias, can undergo a transition to the bubble superstructure (two-dimensional array) state. This transition takes place in the process of gradual cooling from a high-temperature state to low temperatures in specific ranges of electric field magnitudes and temperatures [15]. Moreover, in Ref. [15], an extended set of topologically distinct patterns was reported for *E*-field magnitude varying from zero to the values corresponding to a monodomain state. Also, some insights into specifics of the transitions between topologically distinct states, taking place in low-dimensional ferroelectrics, subjected to an external electric field of varying magnitude, were provided in Ref. [15]. Further studies focusing on the ensembles of electric bubbles reported a prediction of a quasi-hexagonal arrangement of the topological features in ferroelectric $PbTiO_3$ ultrathin films [16]. The work implemented phase-field simulations, with the free energy approximation taken in the Landau-Ginzburg-Devonshire form. Very recently, a similar approach was employed to propose a possible means to control formation and properties of electric bubbles and their corresponding ensembles [17,18]. One of the most important aspects of these studies regards the phenomenon of

induced formation of electric bubbles in ferroelectric thin films via construction of regularly-distributed and weakly correlated artificial electric bubble arrays [17,18]. Moreover, it was shown that these topological features can be controlled by local electric and mechanical stimuli [19]. The effects of quantum fluctuations on the stability of topological textures in ultrathin $Pb(Zr_{0.4}Ti_{0.6})O_3$ ferroelectric films were recently investigated too [20]. It was shown that quantum fluctuations stabilize the topological states within a wider range of external field amplitude, in contrast to expectation that zero-point phonon vibrations should suppress the occurrence of polar phases.

The main focus in the present work is the *physical nature of transition* to bubble states in electric dipole systems, and their thermal behavior away from and around the transition point. Specifically, dynamical behavior around the critical point and major factors leading to the development of instability and transition to a topologically non-trivial state are of particular interest. In the bulk anti- and ferroelectric materials, the transition from a ferroelectric to paraelectric state is known to occur due to softening of one of the optical modes [21,22]. However, in the past, only a few studies have focused on the problem of dynamical behavior of topological states in non-bulk materials. In Ref. [23], the existence of *toroidic modes* in the systems of square $BaTiO_3$ nanowires, embedded in a $SrTiO_3$ matrix, was reported. These toroidic modes were found to demonstrate a softening near transition to electric vortex state, thus implying that the transition is associated with thermal behavior of toroidic excitations. More recently, soft modes have been also reported in systems featuring polar vortex tube states [8,24]. Specifically, regular arrangements of polar vortices in $(PbTiO_3)_n/(SrTiO_3)_n$ superlattices known as vortex crystals were shown to give rise to collective modes (vortexons) that can be described as phonon-like transverse oscillations of polar vortices [8]. The same study revealed that strain-driven softening of vortexons at a fixed temperature can give rise to a static zig-zag vortex pattern. Additionally, a recent study showed that even the formation of vortex tube crystals upon cooling is driven by the softening of finite wavelength phonons coined “vortex waves”. Thereby, the formation of vortex tube crystals and labyrinths was associated with the classical continuous symmetry breaking mechanism.

At the same time, much less is known about the formation dynamics of electric bubble ensembles. The collective dynamics of electric bubbles were investigated in Refs. [20,25,26]. Particularly, Ref. [25] predicted that electric bubbles in PZT-based systems can become highly mobile at elevated temperatures and possess finite life-times thereby giving rise to a liquid-like state. Similar features were later predicted for dilute bubble states in $PbTiO_3/SrTiO_3$ systems [26]. Interestingly, dynamical bubble states driven by quantum rather than thermal fluctuations were also reported [20]. Further understanding of dynamical behavior of topological ferroelectrics is of crucial importance from at least two major perspectives. Firstly, dynamics is known to control the formation of topological textures and phase transitions in bulk and low-dimensional ferroelectrics. As pointed out above, soft-modes play defining role in the processes leading to transitions between distinct states. Secondly, collective dynamics of vortices involves terahertz-level frequencies, and thus, can be of relevance for ultrafast data processing. However, both understanding topological transition and developing terahertz devices require a substantial work to be done on various aspects of inter- and intra-vortex dynamics, and development of methods for tuning dynamical properties by external stimuli.

In the case of magnetic Skyrmion systems, a remarkable progress has been made to date in understanding both thermal stability and behavior [27-34]. The observed thermal behavior was found to differ substantially for ferromagnetic and antiferromagnetic topological features, and, in particular, significant differences were found between isolated Skyrmions on tracks and magnetic Skyrmion superstructures. Interestingly, in some magnetic multi-Skyrmion systems, individual

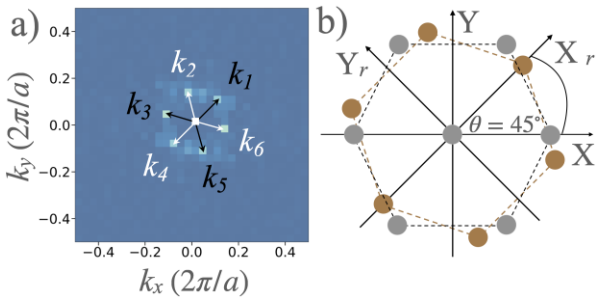


Fig. 1. Characteristics of the reciprocal-space pattern of electric bubble superstructure: a) two-dimensional Fast Fourier Transform (FFT) of the *z*-component of electric dipole field is plotted to emphasize the existence of a quasi-hexagonal lattice order with the equimagnitude wave-vectors, $\vec{k}_i$, $i \in [1,\ldots,6]$; b) the rotation of the quasi-hexagonal superstructure of electric bubbles with respect to the reciprocal of the simulation cell vectors is illustrated. In general, rotation angle, θ, is a function of the electric field. In the considered case, $\theta = 45°$.

topological features were found to arrange into quasi-hexagonal superstructures [35-37]. A complete understanding of the underlying mechanism of the superstructure formation and dynamical evolution is yet to be achieved though. This includes the effects of inter-Skyrmion interactions [38,39], and other factors, which give rise to a (meta-)stable quasi-hexagonal arrangement of individual topological features.

In this work, we investigate the thermal evolution of electric dipole systems during gradual cooling and heating. Under gradual cooling, the system undergoes a transition to a state, wherein quasi-hexagonal ensembles of electric bubbles are formed due to *a concurrent development and evolution of soft-mode triples*, which have the same frequencies. These triplets become frozen-in at the transition point, which is presently close to the room temperature. We investigate the thermal behavior of these soft-modes frequencies and discover that they show a characteristic critical behavior near the transition point. Also, we reveal that the thermal behavior of the parameters, characterizing the degree of ordering in the systems, has similar critical behavior near the transition point. In the low-temperature limit (T = 10 K), the short-range ordering in the systems of electric bubbles was recently investigated in Ref. [40]. Also, in this reference, we discuss the issue of breaking of the long-range order in the systems of electric bubble superstructures.

Modus operandi and model system—We studied the topological transition, thermal and vibrational behavior of the quasi-hexagonal arrays of electric bubbles using an *ab initio*-based molecular dynamics method. We considered a (001)-oriented $PbZr_{0.4}Ti_{0.6}O_3$ (PZT) ultra-thin film deposited on a strontium titanate ($SrTiO_3$) substrate. The PZT thin film is comprised of h_{PZT}= 5 (001)-oriented atomic layers, with both substrate and vacuum interfaces corresponding to Pb-O atomic planes. The growth of PZT ultra-thin film on $SrTiO_3$ substrate is modeled by applying a homogeneous compressive strain of $\approx -2.0\%$ to PZT film. Periodic boundary conditions (PBC) are applied along the *x*- and *y*-axes to the simulation supercell, that are chosen along the [100] and [010] crystallographic directions, respectively. The system lacks periodicity in the *z*-direction and the three dimensions of the simulation supercell are chosen as $32\times32\times h_{PZT}$ lattice units (l. u.). Note that, in Ref. [40], the authors discuss effects of lateral dimensions of the simulation system on the properties of electric bubbles and their quasi-ordered superstructures. It was reported that the orientational order parameter demonstrates behavior characteristic for quasi-ordered structures. The observed lack of long-range order is consistent with experimental observations, reported to date [9,10] (a discussion of magnetic Skyrmions is given in Ref. [41]). The breaking of long-range order was found to occur as a result of formation of electric-bubble polycrystals with two-dimensional crystallites having different rotation angles was tested by varying the size of the simulation supercell. In the study of Ref. [40], simulation systems with dimensions of 56×56×5 and 64×64×5 lattice units were employed. These sizes are sufficient to observe domains with

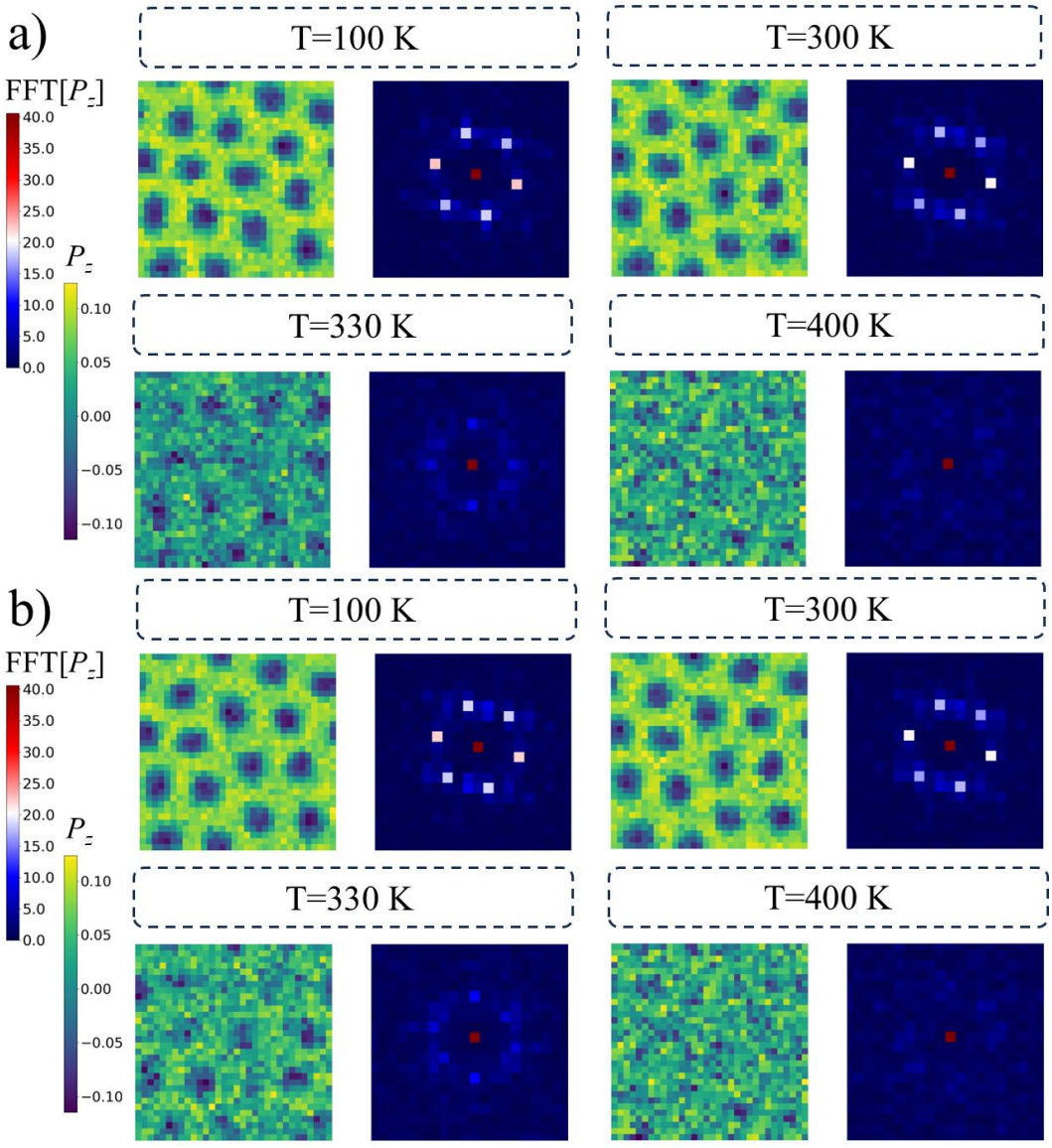


Fig. 2. An illustration of the thermal evolution of the electric bubble patterns during gradual cooling from the high temperature state to T = 10 K (a) and heating from the low temperature state, T = 10 K, to a monodomain state (b) of the dipole configuration subjected to the electric field, E = 40.0×10^7 (V/m). In both cases of temperature variation, the plots show patterns of the z-components of dipoles and 2D FFT of z-components of dipole fields. The results for the dipole systems at temperatures: 1) 100 K; 2) 300 K; 3) 330 K; and c) 400 K are marked in the figure.

different orientations. The screening (surface-induced-charge) parameter is realistically fixed at 0.8 throughout the study. To study the dynamical evolution of the systems under consideration, we used an in-house molecular-dynamics code, based on the effective Hamiltonian model. Details of the simulation method were previously described in Refs. [34,42,43]. In brief, the effective Hamiltonian was parameterized using first-principles calculations, as detailed in Refs. [44,45]. The simulation procedure, employed for studies of temperature dependence of the electric bubble characteristics and thermal properties of superstructures, consists of the following steps. First, the

electric dipole configurations were thoroughly equilibrated at high temperature of 800 K. An external electric field was applied to the simulation system in the *z*-direction, with the magnitude of the field being fixed at $E = 40.0\times10^7$ (V/m). Under these conditions, the topological low-temperature state corresponds to a quasi-hexagonal array of electric bubbles. Further details of the implementation of the molecular-dynamics method are available in Supplemental Material (see Sections SM.1) [46] (see also references [47-53] therein). The soft-mode frequencies were deduced from Spectral Energy Density functions, as described in the Section SM. 2 of Supplemental Material.

Quasi-hexagonal superstructure formation—A brief overview of the topological states unraveled in this work is as follows. For a zero *E*-field magnitude, and in general, for $E \in [0,18] \times 10^7$ (V/m), a quasi-one-dimensional stripe arrays (also known as vortex-tubes [13]) are formed. The case of stripe crystals was previously discussed in detail in Ref. [24], wherein, it was demonstrated that the formation of quasi-one-dimensional vortex-tube crystal state takes place as a result of development of a single soft-mode at temperatures well above the transition. We find that, when the *E*-field magnitude is in the range, $E \in [20,54] \times 10^7$ (V/m), the topological state changes to that of two-dimensional quasi-hexagonal arrays of electric bubbles. As we show below, a similar to vortex-tube crystal soft mode-based mechanism (albeit, much more complex) is responsible for the formation of two-dimensional superstructures of electric bubbles. In this case, *triplets* of *equifrequency* soft-modes emerge in the system, with the corresponding wave-vectors forming an equilateral triangle. In Fig. 1(a), we show the structure factor, obtained for the dipole system, gradually cooled under the external *E*-field, $E = 40.0 \times 10^7$ (V/m). The figure shows a triplet of *equimagnitude* wavevectors (and their opposites); these three modes are formed well above the transition temperature and condense (became frozen-in) at temperatures near the transition point. The three corresponding wavevectors satisfy the following relation: $\vec{k}_1 + \vec{k}_3 + \vec{k}_5$. The same relation holds for the opposite vectors: $\vec{k}_2 + \vec{k}_4 + \vec{k}_6$. These two sets of wave-vectors are drawn in Fig. 1(a) alongside the structure factor. Note that these wave-vectors have numerically the same norm, $|\vec{k}_i| = k_{sm}$, where k_{sm} thus denotes a constant (at a fixed magnitude of the *E*-field) norm of *each* soft-mode wavevector. Correspondingly, the two-dimensional energy surface possesses six energy minima located at points associated with the soft-mode wavevectors: $\pm\vec{k}_1, \pm\vec{k}_3, \pm\vec{k}_5$ (and six for the symmetric counterparts of the above wavevectors). Note that, at the considered herein *E*-field magnitude, the superstructure is rotated with respect to the simulation supercell reciprocal vectors by an angle $\theta = 45°$, as illustrated in Fig. 1(b). The rotation is associated with development of what can be called "grain boundaries" in the systems of quasi-two-dimensional superstructures, and the properties of the ordered (in the short-range sense) quasi-hexagonal arrays depends on those of the individual features and many-body effects (*i.e.*, three- and higher-body interactions; for magnetic Skyrmions, see, for example, Refs. [54,55]). The effects of many-body interactions, in the electric dipole systems, however, remain to be fully understood. The hypothesis that the rotation of the superlattice is a result of long-range border breaking by formation of electric bubble "polycrystals" with two-dimensional crystallites having different rotation angles was tested by variation in the simulation system size (*e.g.*, a system with dimensions of $56\times56\times h_{PZT}$ lattice units was employed).

Thermal transitions during heating and cooling—The evolution of the dipole ensembles in the process of temperature variation was investigated for the cases of gradual cooling and heating. The evolution of the system during gradual cooling from the high temperature state to $T = 10$ K is

illustrated in Fig. 2(a). This case corresponds to the transition from a monodomain state ($T > T_c^c$) to a topologically non-trivial state ($T < T_c^c$), where T_c^c is the transition temperature in the process of cooling. The reverse process, in which the quasi-hexagonal array of electric bubbles is heated from T = 10 K to above the critical point ($T = T_c^h$) and undergoes a transition to the monodomain state ($T > T_c^h$), is illustrated in Fig. 2(b). From a comparison of Figs. 2(a) and 2(b), it can be inferred that in both cases of thermal evolution, the transition between electric bubble and monodomain states takes place at temperatures $300 < T_c^c \approx T_c^h < 330$ K. During cooling, when temperature approaches $T = T_c^c$, local-mode waves (corresponding to soft-mode excitations) become frozen-in and the fixed orientation of the wavevectors emerges. No further evolution of the rotation angle takes place in the temperature range below T_c^c. One can observe only thermal fluctuations with

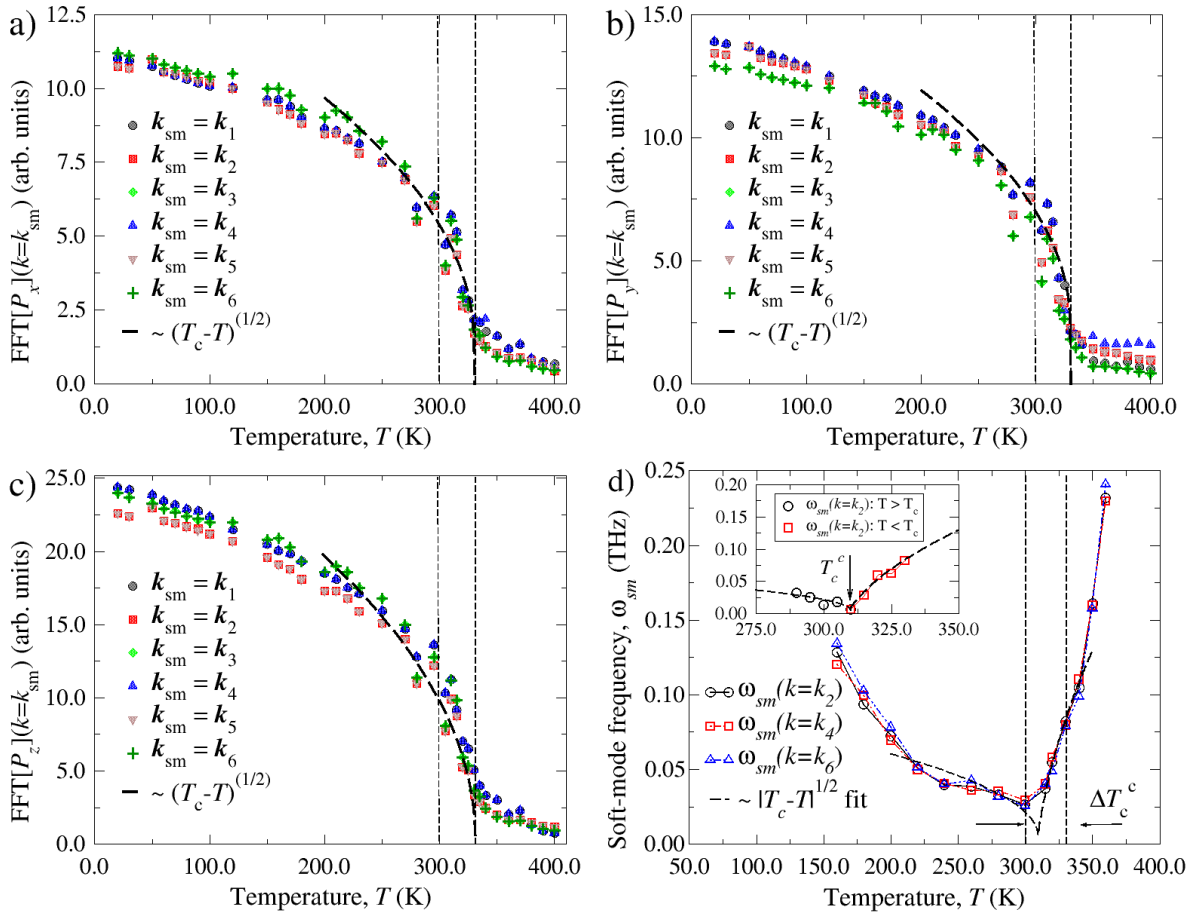


Fig. 3. Degree of order in the system of quasi-hexagonal electric bubbles, represented by the Fast Fourier Transform (FFT) of the three components of polarization vector, (P_x, P_y, P_z), are plotted as a function of temperature: (a) FFT[P_x], computed at the wave-vectors $\boldsymbol{k} = \boldsymbol{k}_{sm}$, is shown. The cases of $\boldsymbol{k}_{sm} = \boldsymbol{k}_i$, $i \in [1,6]$ are plotted separately; (b) FFT[P_y], computed at the wave-vectors $\boldsymbol{k} = \boldsymbol{k}_{sm}$, is shown. The cases of $\boldsymbol{k}_{sm} = \boldsymbol{k}_i$, $i \in [1,6]$ are plotted separately; FFT[P_z], computed at the wave-vectors $\boldsymbol{k} = \boldsymbol{k}_{sm}$, is shown. The cases of $\boldsymbol{k}_{sm} = \boldsymbol{k}_i$, $i \in [1,6]$ are plotted separately. Panel (d) shows temperature dependence of the vibrational soft-mode. In all plots, the results are obtained for systems of electric bubbles, subjected to the E-field, $E = 40.0 \times 10^7$ (V/m). The frequencies are computed for three wave-vectors, which correspond to the rotated basis vectors of reciprocal lattice [see Fig. 1(a)-(b)]. The fits to experimental data near the transition region (marked by two vertical dashed lines) is shown as dashed lines (see text for discussion of the fit). The inset to the panel (d) shows the high-resolution simulation data for $\boldsymbol{k}$=$\boldsymbol{k}_2$ and the square root fitting in the region near the transition point. Also shown in the inset is the transition point, T_c^c, obtained from the soft-mode behavior.

average magnitude of these fluctuations being a decreasing function of temperature. Moreover, a visual inspection allows one to conclude that the radii of the electric bubbles and their arrangement do not significantly evolve in the low-temperature range, far away from $T_c^c \approx T_c^h$. We further note that the specifics of the dipole system at a fixed temperature are similar in the cases of cooling and heating. Thus, at this level of analysis, we find *no signs of thermal hysteresis* in the system.

Temperature dependencies of ordering and soft-mode frequencies—In Fig. 2, thermal evolution of the dipole system is illustrated for the processes of gradual cooling (a) and heating (b). This allows one to hypothesize that the system demonstrates a critical behavior, and the transition to the quasi-ordered state takes place in the temperature range, $T \simeq$300-330 K. First, let us consider the thermal behavior of the degree of hexagonal ordering. One way to quantify the degree of ordering and its variations is to consider the Fast Fourier Transform (FFT) of the local-mode vectors Cartesian components as a function of temperature. Correspondingly, in Fig. 3 (a) through (c), we show the results for $FFT[P_\alpha]$, where P_α, $\alpha = (x, y, z)$, are the Cartesion components of the polarization (local mode) vector, computed in a range of temperatures, above and below the transition point during cooling, for the wavevectors, $\vec{k}_i$, i=[1,…,6], corresponding to the soft-mode triples and their opposites [see Fig. 1(a)]. The behavior of the three components bears a qualitative similarity and the following relation holds: $FFT[P_z] > FFT[P_{x(y)}]$. In the limit of high temperatures and far from the transition point, the dipole system is largely in a monodomain state. This manifests itself in a degree of order being negligible. However, some degree of order is present in the range of temperatures, $T > T_c^c$, as also follows from Fig. 2(a) through (c). This is due to temporally-evolving local-mode fluctuations in the form of developing soft-mode waves, which can, however, be affected by the finite-size nature of the simulation system.

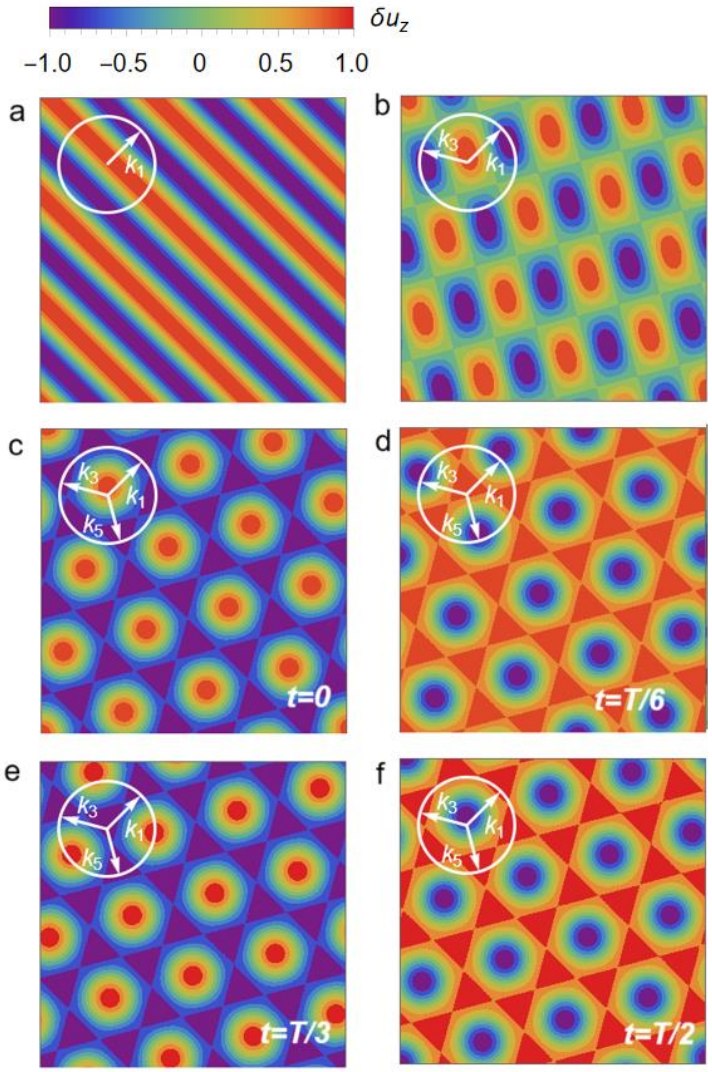


Fig. 4. Dipole vibration patterns corresponding to (a) a single vortex wave with the propagation vector $\vec{k}_1$ (b) superposition of the $\vec{k}_1$ and $\vec{k}_3$ vortex waves with equal amplitudes and (c) superposition of the three equal amplitude vortex waves propagating along $\vec{k}_1$, $\vec{k}_3$ and $\vec{k}_5$. All panels show the schematic distribution of the z components of the dipole displacement vectors at time *t=0*. Panels (d), (e), and (f) show the snapshots of the same wave superposition as panel (c) but one, two and three sixths of the period *T* later; *i.e. t=T/6*, *t=T/3* and *t=T/2*, respectively.

They cause temporal fluctuations in the instantaneous order with non-zero averages. Indeed, note that "unfrozen" soft-modes emerge in the system well above the transition point. The rapid growth of ordering in the system takes place in a narrow transition region, which separates the monodomain state and that, where the quasi-ordered array of electric bubbles is formed. Note that the behavior is affected by the finite-size effects, which is characteristic for numerical studies of critical phenomena. Interestingly, in a range around the transition point, the behavior is characteristic for criticality pertained to phase transitions (as described by the Landau theory of phase transitions). Indeed, as Fig. 3(a) through (c) shows, the behavior is well-approximated by the $FFT[P_\alpha] \sim \sqrt{T_c - T}$ relations for all the polarization vector (soft-mode) components, α. With further lowering of temperature, the degree of ordering further increases, with a flattening of thermal dependence observed in the range of temperatures $10 < T < 200$ K. The differences between $FFT[P_x]$ and $FFT[P_y]$ values in Figs. 3(a) and 3(b) are due to the fact that formation of electric bubbles can be considered as a result of the *E*-field induced decomposition of stripes into bubbles. If such a decomposition is incomplete, it implies a symmetry breaking between *x*- and *y*-directions.

To explore the *dynamical* nature of transition from a high-temperature state of electric dipoles to a quasi-hexagonal electric bubble superstructure (topological) state, we investigated the thermal behavior of the soft modes, associated with the formation of quasi-hexagonal arrays via collective thermal fluctuations in the systems of electric dipoles. Based on the above, we propose that the transition to the quasi-hexagonal state is driven by the short-wavelength soft-mode triples development and condensation. In the considered case, a set of three soft-modes has wavevectors, $\vec{k}_i$; i = (2,4,6), such that the $\vec{k}_2 + \vec{k}_4 + \vec{k}_6 = 0$ relation holds [see Fig. 1(a) for details and notations]. In Fig. 3(d), we show the temperature dependences of the frequencies of these three soft-modes (that are basically equal to each other at any temperature). The dependences were obtained in the range of temperatures from T = 150 K to T = 350 K, thus covering the transition region from the monodomain state to the quasi-hexagonal array state and *vice versa* during gradual cooling and heating. The behavior of the three soft-mode frequencies with temperature is characterized by a decrease in the range $150 \leq T \leq 320$ K. A rapid decrease with T, observed at lower temperatures ($10 < T < 200$ K), changes to a sublinear behavior near the transition point. A well-pronounced minimum is observed at $T \approx$ 310-315 K. At temperatures above the critical one, a sublinear growth in the range around T_c^c is observed; it followed by a rapid increase in the frequencies with temperature, when T >330 K; wherein the behavior is characterized by a growth much faster than sublinear. This is a "mirror reflection" of the case of low T. In the range of temperatures around the transition point, we quantified the critical behavior by fitting the simulation data to the $\omega_{sm} \sim \sqrt{|T_c - T|}$ analytical form. The fits are shown in the figure as dashed lines and further elaborated in the inset to the figure for temperature ranges above and below the transition point. The analytical form is clearly a good representation of the simulation data. Note that, the critical behavior around T_c^c bears a close *qualitative* resemblance with soft-mode behavior in ferroelectric bulk materials [23,56].

To further elaborate the nature of dipole-lattice excitations, we analyzed the eigenvector patterns computed at the soft-mode frequencies above and below the transition point. In both cases, we find that the lowest frequency excitations correspond to a superposition of vortex-like waves [24] propagating along each of the $\vec{k}_i$ wavevectors with eigenvectors $\vec{e_i}$ giving rise to a sequence of polar vortex tubes horizontally stacked along $\vec{k}_i$. For each wavevector, $\vec{k}_i$, the deviation of the dipole α from its equilibrium value is given by a combination of forward, $A_{i\alpha}^{+}\, \vec{e}_i^{\alpha} cos\left(\vec{k}_i \vec{r} - \omega t +\right.$

$\phi_{i,\alpha}^{+}$), and backward, $A_{i\alpha}^{-}\vec{e}_i^{\alpha}cos(\vec{k}_i\vec{r}+\omega t+\phi_{i,\alpha}^{-})$, dipole-lattice vibrations propagating in opposite directions. Here, $A_{i\alpha}^{\pm}$ and $\phi_{i,\alpha}^{-}$ denote the amplitude and the phase, respectively. Figures 4(a) and 4(b) schematically show an example of a $t=0$ snapshot of the polar excitation, formed by a single forward propagating soft-mode wave and a linear superposition of two soft-mode waves with equal amplitudes, respectively. The former excitation gives rise to cycloid-like dipole oscillation, typically associated with nano-stripe patterns [24], while the latter yields a rectangular lattice pattern wherein purple (red) colors highlight the areas of dynamically decreasing (increasing) *z*-component of the dipoles [see Fig. 4(a) and (b)]. These patterns rigidly shift with time along the $\vec{k}_1$ vector for the case of Fig. 4(a) and along $\vec{k}_1+\vec{k}_3$ in case of Fig. 4(b) [see Supplemental Material, Movies 1 and 2]. Adding a third forward propagating mode with wavevector $\vec{k}_5$ gives rise to a more intricate collective excitation. The corresponding map of dipole deviations oscillates between three hexagonal bubble lattices consequently shifted in the direction of $\vec{k}_1$, $\vec{k}_3$ and $\vec{k}_5$ vectors; each one sixth of the period $T/6=\pi/3\omega$. In addition to such a shift, each $T/6$ time the signs of dipole deviations are inverted. Figures 4(c)-(f) illustrate the soft-mode mechanism of the translational symmetry breaking, which underlies the formation of hexagonal bubble lattices. For a perfect hexagonal structure below T_c, the $\vec{k}_i$ points of the unfolded Brillouin zone become symmetry equivalent mapping to the superstructure zone center Γ, which constrains the relative amplitudes $A_{i\alpha}^{\pm}$ and phases $\phi_{i\alpha}^{\pm}$.. In this case, the superposition of forward and backward propagating vortex wave triplets gives rise to low-frequency lattice excitations akin to standing waves. For instance, similarly to the case of the vortex crystals [24], the corresponding excitations lead to coherent oscillations of the dipole amplitude at Γ and "breathing" bubble modes at the superstructures' zone boundary. In contrast, in the vicinity of T_c, the dynamical superposition of unconstrained forward and backward soft-mode triplets allows for bubble shifts [Figs. 4(c)-(f)], which gradually restore translational symmetry and yield a dynamical liquid-like state [24,25] upon further heating. The above analysis further confirms the conclusion that a combination of a soft-mode triplet results in the formation of hexagonal superstructure.

Summary and conclusions—In summary, we have studied topological transitions taking place in ferroelectric ultra-thin $PbZr_{0.4}Ti_{0.6}O_3$ films, subjected to an electric field bias, in the case, when the low-temperature state corresponds to a quasi-hexagonal array of electric bubbles. The transitions in the process of heating and cooling occur here at approximately the same (near 300K) temperature. We found that the topological superlattice formation takes place as a result of development and evolution of *equifrequency* soft-mode triples with linearly dependent wavevectors having equal norms. These three modes arise above the transition point and become frozen-in at near the transition point. The temperature dependence of the soft-modes frequencies in the regions above and below the transition point follows the analytical behavior that is consistent with the predictions of the Landau theory of phase transitions. Correspondingly, the concept of soft modes, characteristic for bulk ferroelectrics, also applies to electric bubble systems. In this case, however, condensation of soft-mode *triples* is responsible for superstructure formation. A similar critical behavior is observed for the degree of order in the electric bubble array. The analysis of eigenvectors provides yet another proof that the soft-modes singles and triples are behind the stripe and quasi-hexagonal superlattice topologies, respectively. The results, reported herein, can be of interest for understanding the role of dynamics in topological structure formation and use of ferroelectric-based material system in the novel devices, wherein functionality is based on local structure manipulation by external stimuli.

Acknowledgements—We acknowledge the Vannevar Bush Faculty Fellowship (VBFF) Grant No. N00014-20-1-2834 from the Department of Defense. The simulations, reported on herein, were performed using the Arkansas High Performance Computing Center.

References

[1] N. D. Mermin, Topological theory of defects in ordered media, Rev. Mod. Phys. **51**, 591 (1979).
[2] G. Catalan, J. Seidel, R. Ramesh, and J. F. Scott, Domain wall nanoelectronics, Rev. Mod. Phys. **84**, 119 (2012).
[3] S. S. P. Parkin, M. Hayashi, and L. Thomas, Magnetic domain-wall racetrack memory, Science **320**, 190 (2008).
[4] Y. Zheng and W. J. Chen, Characteristics and controllability of vortices in ferromagnetics, ferroelectrics, and multiferroics, Rep. Prog. Phys. **80**, 086501 (2017).
[5] J. Junquera, Y. Nahas, S. Prokhorenko, L. Bellaiche, J. Iñiguez, D. G. Schlom, L. Q. Chen, S. Salahuddin, D. A. Muller, L. W. Martin, and R. Ramesh, Topological phases in polar oxide nanostructures, Rev. Mod. Phys. **95**, 025001 (2023).
[6] B. K. Lai, I. Ponomareva, I. I. Naumov, I. Kornev, H. X. Fu, L. Bellaiche, and G. J. Salamo, Electric-field-induced domain evolution in ferroelectric ultrathin films, Phys. Rev. Lett. **96**, 137602 (2006).
[7] P. Zubko, G. Catalan, A. Buckley, P. R. L. Welche, and J. F. Scott, Strain-gradient-induced polarization in SrTiO single crystals, Phys. Rev. Lett. **99**, 167601 (2007).
[8] Q. Li, V. A. Stoica, M. Pasciak, Y. Zhu, Y. K. Yuan, T. N. Yang, M. R. McCarter, S. Das, A. K. Yadav, S. Park, C. Dai, H. J. Lee, Y. Ahn, S. D. Marks, S. K. Yu, C. Kadlec, T. Sato, M. C. Hoffmann, M. Chollet, M. E. Kozina, S. Nelson, D. L. Zhu, D. A. Walko, A. M. Lindenberg, P. G. Evans, L. Q. Chen, R. Ramesh, L. W. Martin, V. Gopalan, J. W. Freeland, J. Hlinka, and H. D. Wen, Subterahertz collective dynamics of polar vortices, Nature **592**, 376 (2021).
[9] Q. Zhang, L. Xie, G. Q. Liu, S. Prokhorenko, Y. Nahas, X. Q. Pan, L. Bellaiche, A. Gruverman, and N. Valanoor, Nanoscale bubble domains and topological transitions in ultrathin ferroelectric films, Adv. Mater. **29**, 1702375 (2017).
[10] S. Das, Y. L. Tang, Z. Hong, M. A. P. Gonçalves, M. R. McCarter, C. Klewe, K. X. Nguyen, F. Gómez-Ortiz, P. Shafer, E. Arenholz, V. A. Stoica, S. L. Hsu, B. Wang, C. Ophus, J. F. Liu, C. T. Nelson, S. Saremi, B. Prasad, A. B. Mei, D. G. Schlom, J. Iñiguez, P. García-Fernández, D. A. Muller, L. Q. Chen, J. Junquera, L. W. Martin, and R. Ramesh, Observation of room-temperature polar skyrmions, Nature **568**, 368 (2019).
[11] V. Govinden, S. Prokhorenko, Q. Zhang, S. Rijal, Y. Nahas, L. Bellaiche, and N. Valanoor, Spherical ferroelectric solitons, Nat. Mater. **22**, 553 (2023).
[12] V. Govinden, S. Rijal, Q. Zhang, D. Sando, S. Prokhorenko, Y. Nahas, L. Bellaiche, and N. Valanoor, Controlling topological defect transitions in nanoscale lead zirconate titanate heterostructures, Phys. Rev. Mater. **5**, 124205 (2021).
[13] V. Govinden, S. Rijal, Q. Zhang, Y. Nahas, L. Bellaiche, N. Valanoor, and S. Prokhorenko, Stability of ferroelectric bubble domains, Phys. Rev. Mater. **7**, L011401 (2023).
[14] Y. Nahas, S. Prokhorenko, J. Fischer, B. Xu, C. Carrétéro, S. Prosandeev, M. Bibes, S. Fusil, B. Dkhil, V. Garcia, and L. Bellaiche, Inverse transition of labyrinthine domain patterns in ferroelectric thin films, Nature **577**, 47 (2020).

[15] Y. Nahas, S. Prokhorenko, Q. Zhang, V. Govinden, N. Valanoor, and L. Bellaiche, Topology and control of self-assembled domain patterns in low-dimensional ferroelectrics, Nat. Commun. **11**, 5779 (2020).
[16] S. Yuan, Z. H. Chen, S. Prokhorenko, Y. Nahas, L. Bellaiche, C. H. Liu, B. Xu, L. Chen, S. Das, and L. W. Martin, Hexagonal close-packed polar-skyrmion lattice in ultrathin ferroelectric PbTiO3 films, Phys. Rev. Lett. **130**, 226801 (2023).
[17] J. H. Ren, L. J. Liu, F. Sun, Q. He, M. J. Wu, W. J. Chen, and Y. Zheng, Spatial modulation strategy for construction of artificial polar skyrmion arrays in ferroelectrics, Phys. Rev. Appl. **22**, 034055 (2024).
[18] J. H. Ren, L. J. Liu, F. Sun, Q. He, M. J. Wu, W. J. Chen, and Y. Zheng, Stabilization and control of weakly correlated polar skyrmions in ferroelectric thin films, Acta Mater. **276**, 120154 (2024).
[19] J. H. Ren, L. J. Liu, F. Sun, Q. He, M. J. Wu, W. J. Chen, and Y. Zheng, Emergence and transformation of polar skyrmion lattices via flexoelectricity, npj Comput. Mater. **10**, 216 (2024).
[20] W. Luo, A. Akbarzadeh, Y. Nahas, S. Prokhorenko, and L. Bellaiche, Quantum criticality at cryogenic melting of polar bubble lattices, Nat. Commun. **14**, 7874 (2023).
[21] C. Milesi-Brault, C. Toulouse, E. Constable, H. Aramberri, V. Simonet, S. de Brion, H. Berger, L. Paolasini, A. Bosak, J. Iñiguez, and M. Guennou, Archetypal soft-mode-driven antipolar transition in francisite CuBi[SeO]OCl, Phys. Rev. Lett. **124**, 097603 (2020).
[22] R. A. Cowley, Soft modes and structural phase transitions, Integr. Ferroelectr. **133**, 109 (2012).
[23] Z. G. Gui and L. Bellaiche, Terahertz dynamics of ferroelectric vortices from first principles, Phys. Rev. B **89**, 064303 (2014).
[24] S. Rijal, Y. Nahas, S. Prokhorenko, and L. Bellaiche, Dynamics of polar vortex crystallization, Phys. Rev. Lett. **133**, 096801 (2024).
[25] S. Prokhorenko, Y. Nahas, V. Govinden, Q. Zhang, N. Valanoor, and L. Bellaiche, Motion and teleportation of polar bubbles in low-dimensional ferroelectrics, Nat. Commun. **15**, 412 (2024).
[26] H. Aramberri and J. Iñiguez-González, Brownian electric bubble quasiparticles, Phys. Rev. Lett. **132**, 136801 (2024).
[27] J. Barker and O. A. Tretiakov, Static and dynamical properties of antiferromagnetic skyrmions in the presence of applied current and temperature, Phys. Rev. Lett. **116**, 147203 (2016).
[28] X. C. Zhang, Y. Zhou, and M. Ezawa, Antiferromagnetic skyrmion: stability, creation and manipulation, Sci. Rep. **6**, 24795 (2016).
[29] D. Cortés-Ortuño, W. W. Wang, M. Beg, R. A. Pepper, M. A. Bisotti, R. Carey, M. Vousden, T. Kluyver, O. Hovorka, and H. Fangohr, Thermal stability and topological protection of skyrmions in nanotracks, Sci. Rep. **7**, 4060 (2017).
[30] S. Rohart, J. Miltat, and A. Thiaville, Path to collapse for an isolated Neel skyrmion, Phys. Rev. B **93**, 214412 (2016).
[31] A. Derras-Chouk, E. M. Chudnovsky, and D. A. Garanin, Thermal collapse of a skyrmion, J. Appl. Phys. **126**, 083901 (2019).
[32] B. Heil, A. Rosch, and J. Masell, Universality of annihilation barriers of large magnetic skyrmions in chiral and frustrated magnets, Phys. Rev. B **100**, 134424 (2019).
[33] A. R. C. McCray, Y. Li, R. Basnet, K. Pandey, J. Hu, D. P. Phelan, X. D. Ma, A. K. Petford-Long, and C. Phatak, Thermal hysteresis and ordering behavior of magnetic skyrmion lattices, Nano Lett. **22**, 7804 (2022).

[34] I. Ponomareva, I. I. Naumov, and L. Bellaiche, Low-dimensional ferroelectrics under different electrical and mechanical boundary conditions: Atomistic simulations, Phys. Rev. B **72**, 214118 (2005).
[35] S. Mühlbauer, B. Binz, F. Jonietz, C. Pfleiderer, A. Rosch, A. Neubauer, R. Georgii, and P. Böni, Skyrmion lattice in a chiral magnet, Science **323**, 915 (2009).
[36] H. Wilhelm, M. Baenitz, M. Schmidt, U. K. Rössler, A. A. Leonov, and A. N. Bogdanov, Precursor phenomena at the magnetic ordering of the cubic helimagnet FeGe, Phys. Rev. Lett. **107**, 127203 (2011).
[37] X. Z. Yu, N. Kanazawa, Y. Onose, K. Kimoto, W. Z. Zhang, S. Ishiwata, Y. Matsui, and Y. Tokura, Near room-temperature formation of a skyrmion crystal in thin-films of the helimagnet FeGe, Nat. Mater. **10**, 106 (2011).
[38] M. Kameda, R. Koyama, T. Nakajima, and Y. Kawaguchi, Controllable interskyrmion attractive interactions and resulting skyrmion-lattice structures in two-dimensional chiral magnets with in-plane anisotropy, Phys. Rev. B **104**, 174446 (2021).
[39] D. Shimizu, T. Nagase, Y. G. So, M. Kuwahara, N. Ikarashi, and M. Nagao, Nanoscale characteristics of a room-temperature coexisting phase of magnetic skyrmions and antiskyrmions for skyrmion-antiskyrmion-based spintronic applications, ACS Appl. Nano. Mater. **5**, 13519 (2022).
[40] M. A. Makeev, S. Rijal, S. Prokhorenko, Y. Nahas, and L. Bellaiche, Quasihexagonal arrays of electric-skyrmion bubbles in thin-film ferroelectrics: Pattern formation and structure, Phys. Rev. B **110**, 144113 (2024).
[41] J. Rajeswari, P. Huang, G. F. Mancini, Y. Murooka, T. Latychevskaia, D. McGrouther, M. Cantoni, E. Baldini, J. S. White, A. Magrez, T. Giamarchi, H. M. Ronnow, and F. Carbone, Filming the formation and fluctuation of skyrmion domains by cryo-Lorentz transmission electron microscopy, Proc. Natl. Acad. Sci. USA **112**, 14212 (2015).
[42] I. Kornev, H. Fu, and L. Bellaiche, Ultrathin films of ferroelectric solid solutions under a residual depolarizing field, Phys. Rev. Lett. **93**, 196104 (2004).
[43] I. Ponomareva, I. I. Naumov, I. Kornev, H. Fu, and L. Bellaiche, Atomistic treatment of depolarizing energy and field in ferroelectric nanostructures, Phys. Rev. B **72**, 140102(R) (2005).
[44] L. Bellaiche, A. García, and D. Vanderbilt, Finite-temperature properties of Pb[ZrTi]O alloys from first principles, Phys. Rev. Lett. **84**, 5427 (2000).
[45] L. Bellaiche, A. García, and D. Vanderbilt, Low-temperature properties of Pb[ZrTi]O solid solutions near the morphotropic phase boundary, Ferroelectrics **266**, 41 (2002).
[46] See Supplemental Material at [URL] for: details of the model implementation; discussion of the methodology of Spectral Energy Density (SED) calculation; additional insights into dynamics of soft-mode waves in the system under consideration. The Supplemental Material also contains Refs. [47-53].
[47] B. K. Lai, I. Ponomareva, I. Kornev, L. Bellaiche, and G. Salamo, Thickness dependency of 180° stripe domains in ferroelectric ultrathin films:: A first-principles-based study, Appl. Phys. Lett. **91**, 152909 (2007).
[48] I. I. Naumov, L. Bellaiche, and H. X. Fu, Unusual phase transitions in ferroelectric nanodisks and nanorods, Nature **432**, 737 (2004).
[49] Y. Nahas, S. Prokhorenko, L. Louis, Z. Gui, I. Kornev, and L. Bellaiche, Discovery of stable skyrmionic state in ferroelectric nanocomposites, Nat. Commun. **6**, 8542 (2015).
[50] D. Sichuga and L. Bellaiche, Epitaxial Pb[ZrTi]O ultrathin films under open-circuit electrical boundary conditions, Phys. Rev. Lett. **106**, 196102 (2011).

[51] L. Lu, Y. Nahas, M. Liu, H. Du, Z. Jiang, S. Ren, D. Wang, L. Jin, S. Prokhorenko, C. L. Jia, and L. Bellaiche, Topological defects with distinct dipole configurations in PbTiO3/SrTiO3 multilayer films, Phys. Rev. Lett. **120**, 177601 (2018).
[52] J. A. Thomas, J. E. Turney, R. M. Iutzi, C. H. Amon, and A. J. H. McGaughey, Predicting phonon dispersion relations and lifetimes from the spectral energy density, Phys. Rev. B **81**, 081411 (2010).
[53] S. O. Sayedaghaee, S. Prosandeev, S. Prokhorenko, Y. Nahas, C. Paillard, B. Xu, and L. Bellaiche, Domain-wall-induced electromagnons in multiferroics, Phys. Rev. Mater. **6**, 034403 (2022).
[54] V. E. Timofeev, A. O. Sorokin, and D. N. Aristov, Towards an effective theory of skyrmion crystals, JETP Lett. **109**, 207 (2019).
[55] I. M. Tambovtsev, I. S. Lobanov, A. D. Kiselev, and V. M. Uzdin, Pair interaction of localized topological structures in confined chiral media, Phys. Rev. E **108**, 024705 (2023).
[56] M. E. Lines and A. M. Glass, *Principles and applications of ferroelectrics and related materials* (Clarendon Press: Oxford University Press, Oxford
New York, 2001), Oxford classic texts in the physical sciences.